Journal of Theoretical and Applied Information Technology
30th April 2020. Vol.98. No 08

ISSN: 1992-8645 www.jatit.org E-ISSN: 1817-3195

STRONG REDUCTION OF SUPER IMAGES BY OPTIMIZING MIXING METHODS AS VECTOR DATA

OLA ALI OBEAD[1], AHMED AL-GHANIMI[2]

[1]al-Mustaqbal University College, Medical Physics Department, Iraq

[2]university Of Babylon, College Of Pharmacy, Iraq.

E-Mail: [1]aliola417@gmail.com , [1]ahmed.h.o.alghanimi@gmail.com

ABSTRACT

The ultra-spectral image set aims to extract the spectra of pure materials from the same scene (the final member bars or orange color), as well as the average amount per pixel of the image. Most algorithms rely on traditional end-organ exploration techniques that often did not work in difficult scenarios. In this work, this problem will be addressed along with the variation of the material by considering that the final member is a direction in the surrounding space which in this case is a one-point substitute. Under this work, we will propose a new algorithm through which we generate a strong reference spectrum. We see the potential of this proposed algorithm which we will apply using real spectra to a set of synthetic data with variability within the class, and the landscape will be the image used.

Keywords: *Hyperspectral mixing, variability of end members, Extended Linear Blend Model, Oblique Variety.*

1. INTRODUCTION

The hyper spectral detection allows an automatic and precise identifications of a material present in a observe scene, fine spectral resolutions of a hyper spectral image **[1].** spatial resolutions are however limiting & a field of sea of the singles pixels often including several material of interest. A spectrum observes are then the mixture of a contribution of a different material present at a location. The Spectral mix is the matter of blinds sources separations whose purposes are to recover a spectra of clear material (it is call end member), & to estimate their relative proportion. (it is call abundance) in each pixels **[2].** The Line Alange (MML) samples [3] are general adopted for these matters. It assume that the pixels of indexed **n** through **N** pixel of a image $x_n \in R^L$, let L is the no. of spectral band used, are decompose to:

$$X_n = \sum_{p=1}^{P} a_{pn} s_p + e_n \quad (1)$$

Let **P** is the no. of material considered, $s_p \in R^L$ is the signature of the end member p, which is supposed to represent perfectly the corresponding material, and $\mathbf{a_{pn}}$ is a coefficienting of abundance of the materials among the pixels n, & $\mathbf{e_n}$ are the additive noises., being of proportion, is subject to a non-negativity of abundances (CNA) constraints and the one-abundance (CSA) constraint, i.e. to say that all pixels should be fully explain by positive contributions from a different material. Geographically, the info are in the simple whose vertices are end members.

MML have been widely use in a last 2 decade, but over a year, some of it is limitation have been identified, name non-flax in a processed of mixing and a variability of material. A first limitation is sensitive in complexity scenarios like the tree canopies plus particulate material (e.g. sand) & require very complexity models of mixing like that bilinear model **[4, 5].** A other side, variability End members are simply a quick that all materials can not be fully representing by the singles spectrum and are always subject to infraclass variation **[6].** These perhaps due to multiple factors, the general one being locally exchanges in illuminations condition (due to shadow and tope graph), and a intrinsic variability of material, correspond to local physicochemical exchanges in their compositions. These variabilities can considerer to a spatial **[7]** and temporal **[8]** domain when it comes to image sequences. Here we focus on variability with the single images. 2 classes of method for remedying them has been identify in **[9]:** "bundle" -depend method, where end members is represents by the collections of signature, possible extract from a info [10], with statistical method, where statistic distribution

ISSN: 1992-8645 www.jatit.org E-ISSN: 1817-3195

assign in end member in allows estimations in all pixels **[11].** Recently, explicit models of variability have been proposed to direct explain a possible variation of end members. **[12, 13].** They share a formulation to the equation (1), except that end member is now index by pixel. 1 like model is a Extend Line Bangle (MMLE) sample, propose in [14]. It approximate Hapke's physical radioactive transfer model [15] into a version exploitable in blind mixing. In [16], a variability of a material due to a illuminations are in fact reasonably explained by positive scale factors depending on the pixel. In its simplest version, the model is written:

$$X_n = \psi_n \sum_{p=1}^{P} a_{pn}\, s_p + e_n \qquad (2)$$

Where ψ_n is the scaling factor that accounts for exchanges in luminosity in pixel spectral signature. In this sample, $\mathbf{s_p}$ is no long from the unique signatures associated with materials p, but rather the references providing directions of the straight lines join a origin and this point, on which find all end members. This formulation led to a fast algorithm for estimating the parameters of this least-squares non-negative model, called Scaled Constrained Least Squares Immixing (SCLSU), view **[13]** for more detail. 'Entails. On the other hand, this algorithm cannot solve other types of variance of the measuring factor. Not all phenomenal changes are taken into account, which are difficult to determine because of the diversity of their causes.

The more complexes versions of MMLE algorithms were discovered [17, 14]. This conclusion takes into account the different scale factor for all materials, but it also allow final members to move the bath from a small copy of the references. , In term of distance Euclidean. For Bayes, this means putting a gaussian a priori on all the local members, centered around copying the reference scale. In this case, the recovered variance is more difficult than just an easy variance of the scale factor and may to some extent explain the effects of fundamental changes. These are done by solve the following optimizations matter:

Let S = {Sn}, n = 1... N with A ΔP that all vectors of abundance ∈ RP in all pixel belong to a simplex part in P vertex, that is, satisfies the CNAs and CSA. pn ∈ Rp × p are diagonal matrices that have a scaling factor based on the material on their diagonal. S0 is the matrices of the reference end members. ||. || F is the Fresenius standard.

The geometric explanation of MMLE in Figure. 1. A information in the convex cone, its edge is terminal ends; with local instance of these (not shown here) is point close to specific location on this line. (References members on a scale). All pixels always belong to simplex.

This structure is useful, but it is directly based on the S0 end members. They must be carefully acquired because they provide convex cone edges, which require the entire mixing process that the Vertex Component Analysis Algorithm (VCA) [18] is best of a most widespread extractions algorithm, based on geometry of a convex matter.

Of pure linear decoration. On the other hand, in cases where shadow or other strong contrast effect is present, this algorithm, which look for extreme point of information, are often retrieved from them. Signature with low capacity (and small signal).

This can explain in a context of a MMLE conical sample. A low-capacity spectrum is close to a origin with return to the shadow; if the sample based on simple geometry is adopted, these points are already extreme in information. These are pieces that represent the spectrum of pure material with cause error in estimating parameters of a mixture.

, we proposed the new formulations of MMLE with the new algorithms to address these problems. We see that uses the model method k and a measure of cosine similarity is

ISSN: 1992-8645 www.jatit.org E-ISSN: 1817-3195

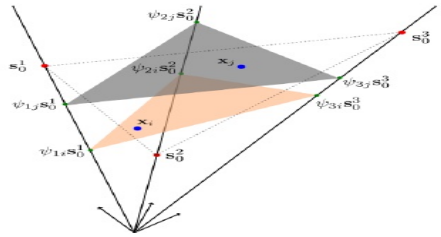

FIGURE 1 - Geometric Interpretations Of A MMLE, As Presenter In [14]. End Member Is Additionally Allowed To Deviate To Benchmark Version Via Gaussian Priors.

Capable of providing relatively reliable initial references signature, which we can refine in a algebra algorithms, by sampling the references end member as directional info, c. 'is to say data that are on the hypersphère unit **[19].** The point on a sphere define in a unique way a directions in a space of the characteristics.

2. PROPOSED SAMPLE AND ALGORITHMS

2.1 Presentation Of A Method

The materials must no longer be summarize by the singles point, but each a points of the line joining a origin and the references represent a same materials, and different luminosity variation. Ideally, the end member must then be view as the directions (or the line among a origin) in s feature space and this in mind, it made more sense for the end member extraction algorithms to look for direction more than extreme point in the info. Finding references direction can be simplied be done use the k-mean algorithm as the preprocess step, with a cosine similarity **cos** d (x_i, x_j)

This measurement is actually insensitive to variables in the size of the spectra. Controversially, we can show that the k method with cosine similarity may be associated with a combination of Von Mises-Fisher distributions (analogical Gaussian distribution of vector information), similar to the fact that the classical k method using the Euclidean distance is associated with a combination of Gaussian distributions [20] which indicate and conclude from this the interest in using the algorithm of means k and cosine similarity in the case of conical models.

Cluster midmost can easily be used as a reference member. However, these may not be excellent with very close to a center of a real convex cone, because a assembly made unique mappings per pixel. This means that the average pixels belonging to the mass tend to be close to the center of the cone due to the effect of similar pixels.

Then it is must to be able to correct this erroneous situation in a interference algorithms. One way to do this in MML is to uses a simplex vole to organize an end organ [21]. However, this regulation is not convex and difficult to treat, and convex relaxations is simple in [22] using the sum of Euclidean spacing between possible pairs of organs, the process of adapting the latter to the conical model of MMLE. It is not easy, since each member can represent at all points on a corresponding lines. The Euclidean distance between any two points on two lines is not suitable to determine the distance between these two lines if we have them with different capacities (as confirmed in a experiment). Spectral angles may be possible, but this amount is difficult to manage in development problem.

To resolve these problems, we suggest modeling reference members as directional's info, that is, as directives in a character space. Eristic. There are many way to do these [23], and the easiest way to restrict a endpoint members to be normal is: || Sp || 2 = 1 ⍱P. In fact, all lines that pass during a original is uniquely positioned with the points on a hypersphère part. Equally, a references referenced matrix must contain columns from Rule 1, ie S0∈ OB (L, P), the so called italic type. [23]. In this case, the distances between a reference on a sphere has a direct effect on the position of the lines: the larger the parameter of the linked organization is (or is small), the closer the straight line is to the line that connects the origin. The average information, with less (or better) accuracy of data. We will see that the position of reference rights (as well as the importance of Gaussian prei on the local member) will also have an impact on the analysis of abundance.

Thus, we are developing MMLE so that we can adjust the reference line positions in the properties area repeatedly. To do this, we suggest reducing the following cost functionality:

ISSN: 1992-8645 www.jatit.org E-ISSN: 1817-3195

$$\underset{A,S,\Psi,S_0}{\operatorname{argmin}} \frac{1}{2}\sum_{n=1}^{N}(\|X_n - S_n a_n\|2^2 + \lambda_s\|S_n - S_0\psi_n)\|F^2) + \frac{\lambda_{So}}{2} tr(S_0 V S_0)$$

s.t $a_n \in \Delta p \forall n b$

$S_0 \in \partial B(L,P)$ (3)

Where we note tr the trace of a matrix, and V = PIP - 1P 1TP (1P, denotes a column vector composed of P 1), so that tr ($S_0VS_0^T$) = $\sum_{i=1}^{p-1}\sum_{j=i+1}^{p} \| (S0i - S0 j) \| 2^2$, that is, the sum of the Euclidean distances between the possible pairs of end members of reference **[22].** λ_S and λ_{S0} are regularization parameters. The term $\lambda_S \| (S_n - S_0 \psi_n) \|^2_F$ force all local end member to be closed to (but not = to) scale version of standard (unit) reference directions. Scale factors capture the variability induced by illumination conditions, whereas S_n can also take into account the effects of intrinsic variability. λ_S is direct relating to the variance of a Gaussian a priori (taken here equally for all end members by simply). A fact that references end members are normalize also have a advantage of making it possible to easily kinds the amplitude of the scale factor (with therefore a impact of the variability induce by illumination) for different material with image. Spatial adjustments can also add if necessary, as are done in **[14]**.

2.2 Optimization However

We developed the algorithms in order to obtain the fixed point from cost functions (4). It is difficult to reduce this objective function because there are many reasons: it is not convex to all variables, which usually require coordinated proportional methods in blocks in order to obtain the locally mini. In these aspects, these approaches are making more difficult cause a matter isn't convex with respect to S0 as well, because of the standard constraints of the unit, which are not convex. On the other hand, we'll saw that can away get the local mini for these variables by take advantages of the Riemannian varietal structures of the constraint sets. Before details a various development step, briefly describe how to configure the algorithms. The k-mean algorithms (with cosine similarity) are first used in order for us to get the cancroids, which we normalize to initialize S0. We configure Sn by setting the appropriate columns from this matrix to the current pixel xn, according to the aggregate label. Other column is initialize use a remaining cancroids. A matrix of abundances with size factors is initialized by using SCLSU algorithms with cancroids as reference, it is best faster. In these ways, it is possible to have the best local mini despite the complexity of amatter.

Development for A is simple. The objective function is discernible, convex, and it is easy to project a set of constraints (simple unity) [24]. We can then get the overall minimum problem for this sub-pixel problem using pixels (for example) descent drop hometown. Developments related to Sn and problemn pose no problem and have analytical solutions (see [17] for details). Developing the S0 level is more difficult due to the constraints of belonging to the unit areas, although the type of objectives is different. Using the fact that the Cod group has a diverse structure of Riemann that enables us to find undoing easilyInitially, we begin to reduce the graduation of communities to diagonal groups. [23] We use the MATLAB Manopt toolbox [25]. The convergence of all sub-problems is guaranteed. We cannot prove the convergence of global algorithms to a specific target point in this case. Moreover, practical convergence is always practical.

The algorithms are discontinued because the relative differences between successive iterations of all variable masses are less than ϵ = 10-3 (in the standard). Note that the convergences will be slow from the original MMLE with the standard fixed-end member, as it is now improved by iteration and will have an impact on the underlying.

3. EXPERIMENTAL RESULTS

In this section, we present the results obtained on a set of synthetic data whose materials comprise and contain realistic spectral variability, as well as parts of the data, with a very correlated final member and large proportions of shaded areas.

3.1 Synthetic Data

DATA GENERATION:

We will first create artificial data sets in the

ISSN: 1992-8645 www.jatit.org E-ISSN: 1817-3195

following way. First, we use the basic facts of the data parts known as the University of Pavia 1 to provide us with so-called spectrum (203 bands in infrared and visible fields). They belong to several parts of the concerns, integrating their spectral fluctuations. We consider 3 parts found in these forms: vegetation, concrete and aluminum roofs. All these parts include both the variability caused by light changes (surfaces and trees with multiple paths relative to the sun) and the sources of fundamental change (especially in concrete and plants). In each pixel, we select the local members as a random pattern in each of these parts (after normalization so that each representative is in the unit field).

The measurement factor was shared using a combination of 4 Gaussian distributions (modified from SCLSU result on sub-images of Pavia information). This reflects the fact that the scale factor often comes from multimedia distribution (such as surfaces with different directions, or shaded areas).

Abundance was shared to be similar, using Dirichlet distributions so that the probability density is centered around the edges and heads of single simplicity (which contain a certain percentage of heavily mixed pixels and all of which are continuous).

The data were also created using equation (2), adding Gaussian noise to make the signal-to-noise ratio 30 dB. The latter picture is then leveraging the reality of these characteristics.

RESULTS:

First, we perform a VCA + SCLSU algorithms to quick obtain spectral variability-based mixing results using end members obtained via VCA. We show below that this approach gives very bad results. Then we focus on the test of 2 algorithm and references obtained via k mean: SCLSU with a MMLE of **[17].** Moreover, we define by MMLE-SDC (Sum of Distance in Square) a increased MMLE of convex regularization on volume, but without the constraint of oblique variability. Finally, we compare each this method to the developed method, called RMMLE (for a robust version of Model of Extended Linear Meelange). Note that don't compare a result with a mixture using the standard Fully Constrained Least Squares Immixing (FCLSU) algorithm **[26],** because this algorithms are depend on a info geometry according to a simple, and has been defeated in multiple scenarios where variability is significant. For all algorithms, we adjust the regularizations parameter empirically to obtain the good possibility performance (the select value is reporter in Table 1). Quantitative result is presented uses 2 measures: the mean square wrong between actual abundance (a EQM) with those estimated: $\frac{1}{n\sqrt{p}}\sum_{n=1}^{N}.\left\|\hat{a}n-an\right\|_2$, and the average spectral angle (on each pixel with material) (SAM for Spectral Angles Mapped)

SAT= $\frac{1}{NP}\ \sum_{n=1}^{N}.\sum_{p=1}^{p} aco \qquad \left(\frac{\hat{s}_{pn}^{T}s_{pn}}{\|\hat{s}_{pn}\|2\|s_{pn}\|2}\right)$

between the real members of each pixel and those that are retrieved. This quantity' collated in Table 1.

VCA and SCLSU approach achieve very poor result together in abundances estimations within variability estimations, the rezones indeed 2 of a extracted signature is associate and pixel and small scales factors. Scales, and have the very low amplitude. Uses k means instead, and SCLSU, lead to better result.

Table 1 - Quantitative results on synthetic information. With the exception of VCA + SLCSU, each algorithm use the k mean to obtain the initial reference matrices. The values of the organization parameters are indicated as needed for these parameters.

	λ_S	λ_{S0}	AE QM	SAM(degrees)	Time (s)
VCA+SCLSU	×	×	0.2056	542	2
SCLSU	×	×	0.0650	6.30	2
MMLE	0.01	×	0.0500	5.58	57
MMLE+SDC	0.1	0.25	0.1710	10.38	1400
RMMLE	0.1	0.5	0.0450	3.46	2240

Away from the best level because the variance is explained only by the measurement factor. The MMLE is good cause of a add Gaussian bias. see a importance of variable oblique constraints on a last 2 rows of the table: MMLE + SDC has failed because the regularity requirements depend on comparing references with potentially different capacities, while introducing constraints leads to good results. . Figure 2 illustrates successful

ISSN: 1992-8645 www.jatit.org E-ISSN: 1817-3195

results using a scattering scheme (by using the first three main components) plus obtaining the final members of the top three algorithms (other schemes show that a line is too far from a real cone not belonging for them). Similar conclusions can draw from this fig, which illustrate that the RMMLE method is able to find a good end organs in each pixel.

3.2 Real Data

By using the CASI-3 sensor (72 spectral bands in the visible field and near infrared [27]. The spatial resolution is 1m. The image we use is a 207 x 268 x 72 group size for the entire scene. RGB representations are see in Fig 3 (a). These inputs set was used for the supervise classifications of tree species, uses fact field information with LiDAR information as the add classifications property, since the different tree type is in this case converging. The image also includes many gray areas due to tree crowns, which were a major problem in previous studies [27]. However, there are other non-plant materials, such as surfaces, roads and ground.

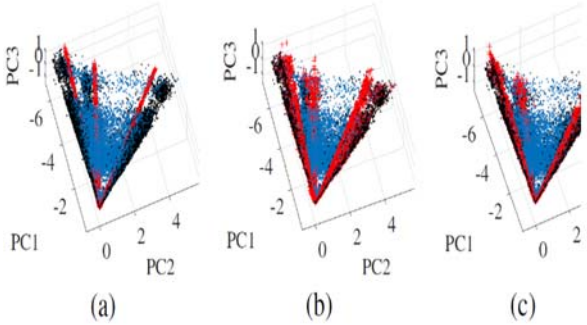

Figure 2 *- Dispersion Of Data (Blue), True End Members (Black) And Those Extracted (Red) For (A) Sclsu (B) Mmle (C) Rmmle.*

Persian of info with clear pixels' shown in the figure 3 (c). We combine info by using P = 4 material with the algorithms mentioned above. Figure 4 shows the scatter plots of data and end members retrieved for VCA + SCLSU, SCLSU, MMLE and RMMLE. Abundance map I s shown in Figure 5. For the MMLE, we use $\lambda_S = 0.02$, and for the RMMLE, we use $\lambda_S = 0.6$ and $\lambda_{S0} = 100$. As in cases of synthetic info, end members recovered by VCA are bad because of the shadows area of images; with a corresponded abundance do not make sense. Same of the info is projecting on the lines closest to the cone mater, which represents vegetations. On the other hand, the use of k-means makes it possible to distinguish conifers from hardwoods. Turf and shadows are also characterized by small and large scale factor values, respectively (scale factors are not see here due to space constraint). An abundances of SCLSU with MMLE is rather like that, slight more parsimonious for the MMLE, because it's able to best capture the effect of variability than SCSLU (as shown in Figure 4 (c). Since RMMLE is able to adjust reference, it is possible to obtain more parsimonious abundance map that correspond closely to a ground truths of Figure 3 (B). We See That The Identify Lines Embrace An Info Set Good Well And Is A Closest To A Field Truth Pixel Of Fig. 3 (C). Fig. 4.

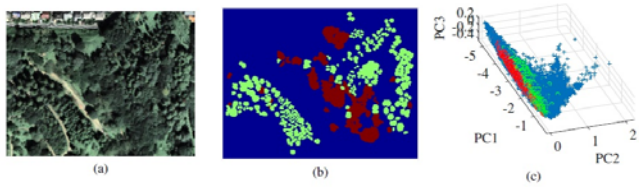

(Green). (C) Dispersion Of Info, And Pixels Of Field Truth (Same Color Code).

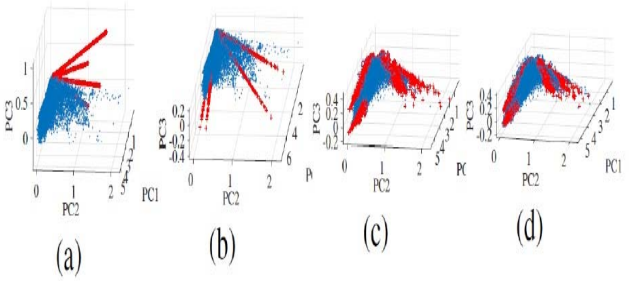

Figure 4 - Dispersion Of Data (Red) And Extracted End Members (Blue) For (A) Vca + Sclsu (B) Sclsu (C) Mmle (D) Rmmle.

ISSN: 1992-8645 www.jatit.org E-ISSN: 1817-3195

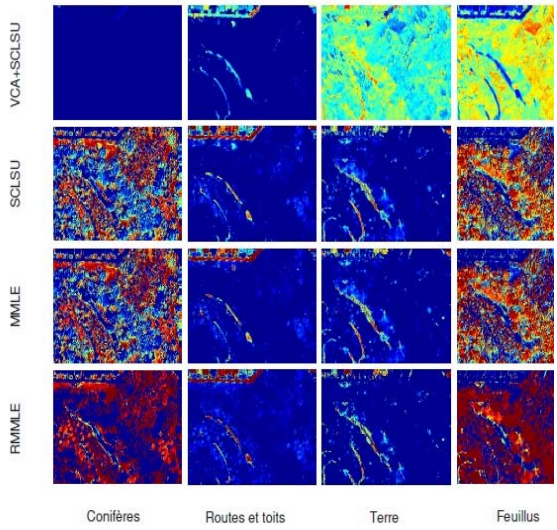

FIGURE 5 - Abundance Maps Obtained By The Tested Algorithms.

4. CONCLUSIONS

We proposed the modren algorithm in this paper for interchanging hyperspectral data, takes into accounts both a variability induced by illumination with a intrinsic variability of end members. the proposed algorithm is able to obtain best reference end members' estimate than VCA take advantage of a factor that end member is well modeled by direct info. The references signature is constrain to be on a level sphere since all points on the latter corresponds complete to the straight lines in the spaces of characteristics. Robust estimate of convex cone edge are obtained as part of the Extended Linear Blend model. The result on the synthetic info sees the relevance of the approaches and the best performances are also proved on a complex truth data set. Related works will include the bath to automatically estimate hardware-dependent parameter (like that Gaussian a priori variance), and tests on a different ways of representing end members in using directional data.

REFERENCES:

[1] J. M. Bioucas-Dias, A. Plaza, G. Camps-Valls, P. Scheunders, N.M. Nasrabadi, and J. Chanson, "Hyperspectral remote sensing data analysis and future challenges," IEEE Geosciences and Remote Sensing Magazine, Vol. 1, no. 2, pp. 6-36, June 2013.

[2] N. Keshava and J. F. Mustard, "Spectral Unmixing," IEEE Signal Processing Magazine, Vol. 19, no. 1, pp. 44-57, Jan 2002.

[3] JM Bioucas-Dias, A. Plaza, Dobigeon N., Parente M., Qian Du, P. Gader, and J. Chanussot, "Hyperspectral unmixing overview: Geometrical, statistical, and sparse regression-based approaches," IEEE Journal of Selected Topics in Applied Earth Observations and Remote Sensing, vol. 5, no. 2, pp. 354-379, April 2012.

[4] R. Heylen, M. Parente, and P. Gader, "A review of nonlinear hyperspectral unmixing methods," IEEE Journal of Selected Topics in Applied Earth Observations and Remote Sensing, vol. 7, no. 6, pp. 1844-1868, June 2014.

[5] N. Dobigeon, J. Y. Tourneret, C. Richard, J. C. M. Bermudez, S. McLaughlin, and A. O. Hero, "Nonli-near unmixing of hyperspectral images : Models and algorithms," IEEE Signal Processing Magazine, vol. 31, no. 1, pp. 82–94, Jan 2014.

[6] B. Somers, G. P. Asner, L. Tits, and P. Coppin, "Endmember variability in spectral mixture analysis: A review," Remote Sensing of Environment, vol. 115, no. 7, pp. 1603 - 1616, 2011.

[7] L. Drumetz, G. Tochon, MA Veganzones, J. Chanussot, and C. Jutten, "Improved local spectral unmixing of hyperspectral data using an algorithmic regularization path for collaborative sparse regression," in Acoustics, Speech and Signal Processing (ICASSP), 2017 IEEE International Conference on. IEEE, 2017, pp. 6190-6194.

[8] S. Henrot, J. Chanussot, and C. Jutten, "Dynamical spectral unmixing of multitemporal hyperspectral images," IEEE Transactions on Image Processing, vol. 25, no. 7, pp. 3219-3232, July 2016.

[9] A. Zare and K. C. Ho, "End member variability in hyperspectral analysis: Addressing spectral variability during spectral unfixing," IEEE Signal Processing Magazine, Vol. 31, no. 1, pp. 95-104, Jan 2014.

[10] B. Somers, M. Zortea, A. Plaza, and G. P. Asner, "Automated extraction of image-based endmember bundles for improved spectral unmixing," IEEE Journal of Selected Topics in Applied Earth Observations and Remote Sensing, vol. 5, no. 2, pp. 396-408, April 2012.

ISSN: 1992-8645 www.jatit.org E-ISSN: 1817-3195

[11] A. Halimi, N. Dobigeon, and J. Y. Tourneret, "Unsupervised unmixing of hyperspectral images accounting for endmember variability," IEEE Transactions on Image Processing, Vol. 24, no. 12, pp. 4904-4917, Dec 2015.

[12] P. - A Thouvenin, N. Dobigeon, and J.-Y. Tourneret, "Hyperspectral Unmixing with Spectral Variability Using a Disturbed Linear Mixing Model," IEEE Transactions on Signal Processing, vol. 64, no. 2, pp. 525-538, 2016.

[13] M. A. Veganzones, L. Drumetz, R. Marrero, G. Tochon, M. Dalla Mura, A. Plaza, J. M. Bioucas-Dias, and J. Chanussot, "A new extended linear mixing model to address spectral variability," in Proc. IEEE Workshop on Hyperspectral Image and Signal Processing: Evolution in Remote Sensing (WHISPERS), 2014.

[14] L. Drumetz, M. A. Veganzones, S. Henrot, R. Phlypo, J. Chanussot, and C. Jutten, "Hyper spectral Blind Unmixing Using an Extended Linear Mixing Model to Address Spectral Variability," IEEE Transactions on Image Processing, Vol. 25, no. 8, pp. 3890-3905, Aug 2016.

[15] B. Hapke, Theory of reflectance and emittance spectroscopy, Cambridge University Press, 2012.

[16] L. Drumetz, Endmember variability in hyperspectral image unmixing, Ph.D. thesis, University of Grenoble Alpes, 2016.

[17] L. Drumetz, S. Henrot, M. A. Veganzones, J. Chanussot, and C. Jutten, "Hyperspectral Blind Unmixing Using an Extended Linear Mixing Model to Address Spectral Variability," in IEEE Workshop on Hyperspectral Image and Signal Processing: Evolution in Remote Sensing (WHISPERS 2015), 2015, pp. 1-4.

[18] J.M.P. Nascimento and J.M. Bioucas Dias, "Vertex component analysis: a fast algorithm to unmix hyperspectral data," IEEE Transactions on Geoscience and Remote Sensing, vol. 43, no. 4, pp. 898-910, April 2005.

[19] K. V. Mardia and P. E. Jupp, Directional statistics, flight. 494, John Wiley & Sons, 2009.

[20] A. Banerjee, I. S. Dhillon, J. Ghosh, and S. Sra, "Clustering on the Hypersphere Unit Using Mises-Fisher Distributions," Journal of Machine Learning Research, Vol. 6, no. Sep, pp. 1345-1382, 2005.

[21] J. Li and J.M. Bioucas-Dias, "Minimum volume simplex analysis: A fast algorithm to unmix hyperspectral data," in Geoscience and Remote Sensing Symposium, 2008. IGARSS 2008. IEEE International, July 2008, vol. 3, pp. III – 250–III – 253.

[22] M. Berman, H. Kiiveri, R. Lagerstrom, A. Ernst, R. Dunne, and J. F. Huntington, "ICE: A statistical approach to identifying end-members in hyperspectral images," IEEE Transactions on Geoscience and Remote Sensing, vol. 42, no. 10, pp. 2085-2095, 2004.

[23] P-A Absil, Robert Mahony, and Rodolphe Sepulcher, Optimization algorithms on matrix manifolds, Princeton University Press, 2009.

[24] L. Condat, "Fast projection on the simplex and the L1 ball," Mathematical Programming, pp. 1-11, 2014.

[25] N. Boumal, B. Mishra, P.A. Absil, and R. Sepulcher, "Manopt, a Matlab toolbox for optimization on manifolds," Journal of Machine Learning Research, vol. 15, pp. 1455-1459, 2014.

[26] D.C. Heinz and Chein-I Chang, "Fully constrained least squares linear spectral mixture analysis method for material quantification in hyperspectral imagery," IEEE Transactions on Geoscience and Remote Sensing, vol. 39, no. 3, pp. 529-545, Mar 2001.

[27] T. Matsuki, N. Yokoya, and A. Iwasaki, "Hyperspectral tree species classification of Japanese mixed complex forest with the aid of LiDAR data," IEEE Journal of Selected Topics in Applied Earth Observations and Remote Sensing, vol. 8, no. 5, pp. 2177-2187, 2015.